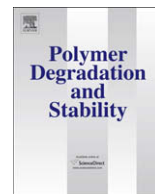




Since January 2020 Elsevier has created a COVID-19 resource centre with free information in English and Mandarin on the novel coronavirus COVID-19. The COVID-19 resource centre is hosted on Elsevier Connect, the company's public news and information website.

Elsevier hereby grants permission to make all its COVID-19-related research that is available on the COVID-19 resource centre - including this research content - immediately available in PubMed Central and other publicly funded repositories, such as the WHO COVID database with rights for unrestricted research re-use and analyses in any form or by any means with acknowledgement of the original source. These permissions are granted for free by Elsevier for as long as the COVID-19 resource centre remains active.



Preparation and characterization of polyoxometalate-modified poly(vinyl alcohol)/polyethyleneimine hybrids as a chemical and biological self-detoxifying material

K.H. Wu^{a,*}, P.Y. Yu^a, C.C. Yang^b, G.P. Wang^b, C.M. Chao^b

^a Department of Applied Chemistry and Material science, Chung Cheng Institute of Technology, NDU, Tahsi, Taoyuan 335, Taiwan

^b Chemical Systems Research Division, Chung Shan Institute of Science and Technology, Lungtan, Taoyuan 325, Taiwan

ARTICLE INFO

Article history:

Received 7 April 2009

Received in revised form

6 May 2009

Accepted 11 May 2009

Available online 21 May 2009

Keywords:

Poly(vinyl alcohol)

Polyethyleneimine

Polyoxometalate

Permeable membrane

Antibacterial effect

ABSTRACT

Nanohybrid membranes based on the Keggin-type polyoxometalate (POM) $H_5PV_2Mo_{10}O_{40}$ and a poly(vinyl alcohol)/polyethyleneimine (PVA/PEI) blend were prepared as a chemical and biological protective material. The objective of the study was to develop and evaluate permeable membranes (PVA/PEI) impregnated with reactive nanoparticles (POM) that can protect against simulants of chemical and biological warfare agents. The physical properties of the PVA/PEI–POM hybrids were examined using SEM, TEM, TGA, and UV–Vis spectroscopy, the results of which indicated that the POM was incorporated in the PVA/PEI matrix after impregnation. The redox properties against 2-chloroethyl-ethyl sulfide (CEES) were investigated based on significant color changes and UV absorption in the POM upon reduction by CEES. The antibacterial effects of the PVA/PEI–POM hybrids were assessed by the zone of inhibition, minimum inhibitory concentration (MIC), and plate-counting methods. The results of this study showed that PVA/PEI–POM hybrids that act against simulants of chemical and biological weapons while retaining their ability to transmit moisture vapor could be obtained.

© 2009 Elsevier Ltd. All rights reserved.

1. Introduction

It has been discovered that the specially-created Defence Science and Technology Laboratory (Dstl) at Porton Down has developed, in collaboration with industry, a novel polymeric material that demonstrates both moisture vapor permeability and chemical barrier properties [1]. This material is composed of two water-soluble polymers, poly(vinyl alcohol) (PVA) and poly(ethyleneimine) (PEI). The selectively permeable material acts as a complete barrier towards toxic liquid, vapor and aerosol challenges yet allows moisture vapor to permeate, consequently representing a leap forward in the area of protective garment design. PVA can be considered a good host material for metals and semiconductors due to its good thermo-stability, chemical resistance and gas barrier properties [2]. Moreover, it contains a carbon backbone with hydroxyl groups attached to methane carbons; these hydroxyl groups can be a source of hydrogen bonding, hence assisting in the formation of polymer blends [3]. PEI is a hyper-branched amine polymer based on aziridine that has widespread

applications in adhesives, coatings, textile manufacture, food packaging and cosmetics. PEI-treated cotton fabric has also been shown by the Dstl to be an excellent scavenger of sulfur mustard (HD) and soman (GD) vapors: this may be attributed to the nucleophilic amine groups, which can react with electrophilic species such as these [4].

Polyoxometalates (POMs) are a large class of metal oxide cluster compounds composed of d^0 transition metal atoms, typically W(VI), V(V), Mo(VI), Nb(V), and Ta(V), bridged by oxygen atoms [5–9]. Many classes of POMs undergo rapid, reversible redox changes. They are of proven value in catalysis and other areas, partly because their extremely versatile redox potentials, acidities, polarities, solubilities, and other properties can be readily altered synthetically. Several types of POM change color when they are reduced. So, if a chemical warfare agent (CWA) with an oxidizable group, such as the sulfur atom in HD or possibly in VX, were to come into contact with the POM–cream mixture, the POM would be reduced (the HD or VX oxidized). Because the reduced POM (POM_{Red}) and the oxidized POM (POM_{Ox}) are different colors, the wearer would therefore have a facile indicator or warning of the presence of the CWA [10–12] – in other words, the agent would be detected by the POM–cream mixture. If the POM in the cream catalyzes the O₂-based oxidation and/or hydrolysis of the CWA, the POM–cream could be catalytically decontaminating as well as detecting.

* Corresponding author.

E-mail address: khwu@ccit.edu.tw (K.H. Wu).

POMs perform significant biological activities with high efficacy and low toxicity. In particular, the sizes and globular structural motifs of many POMs are similar, and in some cases nearly identical, to some water-soluble fullerene derivatives that exhibit fairly good anti-human immunodeficiency virus (HIV) activity [13–15]. So far, various biological effects of POMs have been reported in terms of antitumor and antiviral activities [16,17]. With regard to the antibacterial activity of POMs, we found that polyoxometalates with Keggin, lacunary Keggin, Wells-Dawson, double-Keggin, and Keggin-sandwich structures enhanced the antibacterial activity of β -lactam antibiotics on methicillin-resistant *Staphylococcus aureus* (MRSA) [18], *Helicobacter pylori* [19] and the SARS coronavirus (SARS-CoV) [20–22].

Polyoxometalates supported on porous carbons have been reported to form selective and recoverable heterogeneous catalysts for the rapid room-temperature oxidation of thioether analogues of mustard [14]. Nano-sized metal oxides have been reported to decontaminate chemical warfare agents [23] and can exhibit biocidal activity towards spores of biological warfare (BW) analogues [24]. An iodosobenzoate derivative of β -cyclodextrin (IBA- β CD) has been reported to catalyze the hydrolysis of soman and soman analogues [25]. In laboratory tests, these materials have demonstrated an ability to detoxify and destroy chemical agents and their simulants by breaking down their chemical structure; they have also been determined to be effective in destroying biological agent simulants including virus and bacteria spores in initial tests. In this study, we developed a facile method of immobilizing the POM ($H_5PV_2Mo_{10}O_{40}$) in a PVA/PEI blend to facilitate transport through membranes of PVA/PEI–POM and investigated its permeability, redox properties and antibacterial activity. In order to explore the antibacterial effects of the PVA/PEI–POM hybrids, zone of inhibition testing, minimum inhibitory concentrations (MICs) and the plate-counting method were used in this study to examine the antibacterial activity of the PVA/PEI–POM hybrids against Gram-negative *Escherichia coli* (*E. coli*) and *Pseudomonas aeruginosa* (*P. aeruginosa*), and Gram-positive *S. aureus* and *Bacillus subtilis* (*B. subtilis*).

2. Experimental

2.1. Preparation of PVA/PEI–POM hybrid membranes

PEI of an average molecular weight of 750,000 was purchased from Aldrich as a 50 wt.% aqueous solution. The ratio of primary:secondary:tertiary amino groups in PEI is approximately equal to 1:2:1. PVA (Aldrich, >99% hydrolyzed powder) has an average molecular weight of 89 000–98 000. Polyoxometalate ($H_5PV_2Mo_{10}O_{40}$) was purchased from Japanese Inorganic Chemistry Industry Joint-stock Company and was used as received. 2-chloroethyl-ethyl sulfide (2-CEES, one-armed mustard) was purchased from Aldrich and was used as received.

The PVA/PEI blend and PVA/PEI–POM hybrid membranes were prepared as follows. Doped solutions were prepared by adding a 20 wt.% PEI solution to a 10 wt.% PVA solution. The doped solution was then cast onto a glass plate of a thickness of 1000 nm and placed in a drying oven at 50 °C for 12 h, and the blended membrane was finally obtained by heat-treating the dried membrane at 110 °C for 1 h. The glass plate with the membrane was then immersed in a water bath to detach the membrane. This sample was referred to as the Polymer (PVA/PEI blend). PVA/PEI–POM hybrid membranes were prepared in the same way, except for the fact that a various amounts (about 3–10 wt.%) of POM were added in the preparation step. A POM loading of about 5.0 g was dissolved in 95 mL of water and the resulting solution added to the above-described doped solutions, and stirring was continued under

an inert atmosphere at room-temperature for another 3 h. POMs were produced at concentrations of 3.0, 5.0, 8.0, and 10.0 wt.%; the corresponding PVA/PEI–POM hybrids were designated Polymer/POM-3, Polymer/POM-5, Polymer/POM-8, and Polymer/POM-10, respectively, according to the POM content in the PVA/PEI blend.

2.2. Characterization

The morphology of the hybrids was observed using a scanning electron microscope (SEM, Hitachi S-800) and a transmission electron microscope (TEM, Philips CM-200) equipped with an energy-dispersive X-ray (EDX, Hitachi S-300) microanalysis system. A Perkin–Elmer thermal gravimetric analyzer (TGA-7) was used to investigate the thermal stability of the hybrids. The samples (about 10 mg) were heated in air and under an N_2 atmosphere from ambient temperature to 700 °C at a heating rate of 20 °C/min, and the gas flow rate was maintained at 50 mL/min. The membrane transport of water vapor from the inside to the outside was calculated by the permeation rate (flux, $g/cm^2 h$) in order to measure the water vapor permeation through the Polymer/POM films over a 24 h period at 32 °C. The cumulative mass of vapor permeating the swatch per unit area during the 24 h test was based on the mass permeated in the time interval over the effective swatch area, which was the opening in the permeation cell ($1.1304 cm^2$). The redox reactivities of the Polymer/POM hybrids against CEES were also tested; the experiment was performed in 5 mL of the Polymer/POM solutions containing 0.5 mL of CEES and monitored using a UV–Vis spectrophotometer (UV-3000).

2.3. Test of antibacterial properties

P. aeruginosa (ATCC 27853), *E. coli* (ATCC 25922), *S. aureus* (ATCC 25923), and *B. subtilis* were obtained from the Food Industry Research and Development Institute, Taiwan, and were used as the reference strains in antibacterial testing. The antibacterial spectrum of the Polymer/POM hybrids was evaluated by zone of inhibition testing. A standard inoculum of the test organism with 10^7 colony-forming units (CFU)/mL was swabbed onto the surface of a Muller-Hinton agar plate, and discs of filter paper impregnated with antibacterial agents (6 mg/mL) were placed on the agar. The plates were incubated overnight at 37 °C, and the clear zones around the disc were then measured.

The antibacterial effects of the hybrids were evaluated by the determination of the minimum inhibitory concentration (MIC) using the broth dilution method. Tubes containing 5 mL MH broth with 10-fold dilutions of the Polymer/POM hybrids ranging from 0.002 mg/L to 200 mg/L were inoculated with 10^7 CFU/mL of bacteria. The inoculated tubes were then incubated at 37 °C for 18 h, following that the tubes were examined without shaking for visible turbidity. The MIC was determined as the lowest dilution of composite that produced no visible turbidity [26]. The test was performed three times for each strain, and results in agreement on two or more occasions were adopted as the MIC of the strain.

The plate-counting method was used to further investigate the antibacterial effects of the hybrids [27]. Approximately 10^7 CFU of *S. aureus* were cultured on MH agar plates supplemented with the Polymer/POM-8 hybrids. A Polymer/POM-free MH plate cultured under the same conditions was used as a control. The plates were incubated at 37 °C for 18 h and the numbers of colonies were counted. The test process was as described as follows: 50–400 mg of the Polymer/POM-8 hybrid was added into 3 mL of MH broth containing 10^7 CFU/mL bacteria. The mixture was aerobically incubated at 37 °C under vibration for 24 h; 30 μ L of the above suspension was then cultured on an agar plate and incubated at 37 °C for 18 h.

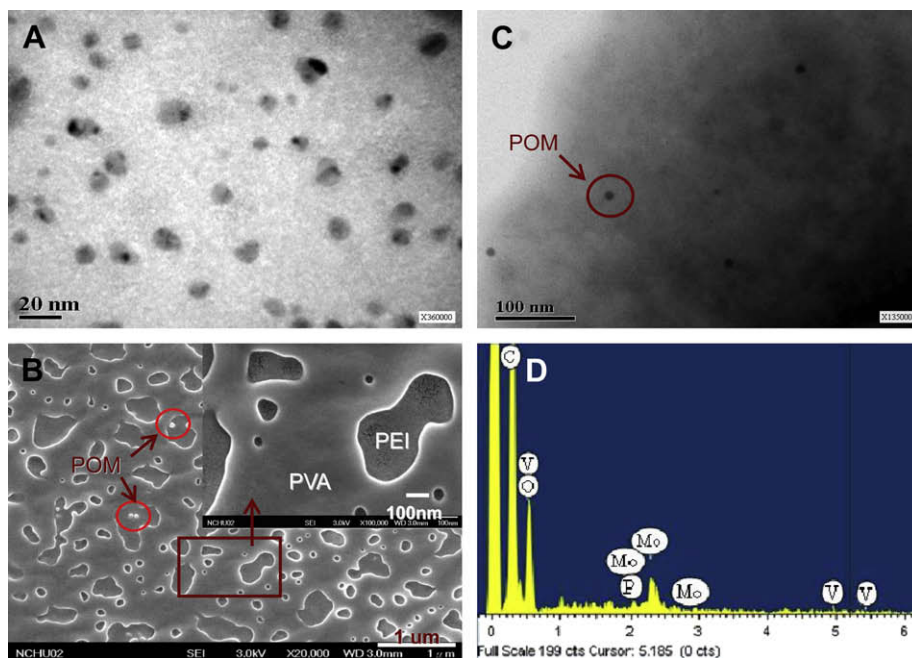


Fig. 1. SEM photographs of (A) POM, (B) Polymer/POM-8 hybrid; (C) TEM photograph and (D) EDX spectrum of the Polymer/POM-8 hybrid.

3. Results and discussion

3.1. Structure characterization

SEM and TEM images were used to evaluate the surface morphology and size distribution of the POM deposited in the

PVA/PEI blend. The SEM image of the Polymer/POM-8 hybrid film showed non-agglomerated, uniformly-distributed POM particles in the PVA/PEI film. The particles are of a spherical nature and seem to be nanosized, typically in the range of <20 nm (Fig. 1A). On the other hand, it was observed that the PVA/PEI blend exhibited a heterogeneous morphology with PEI polymers of micron size

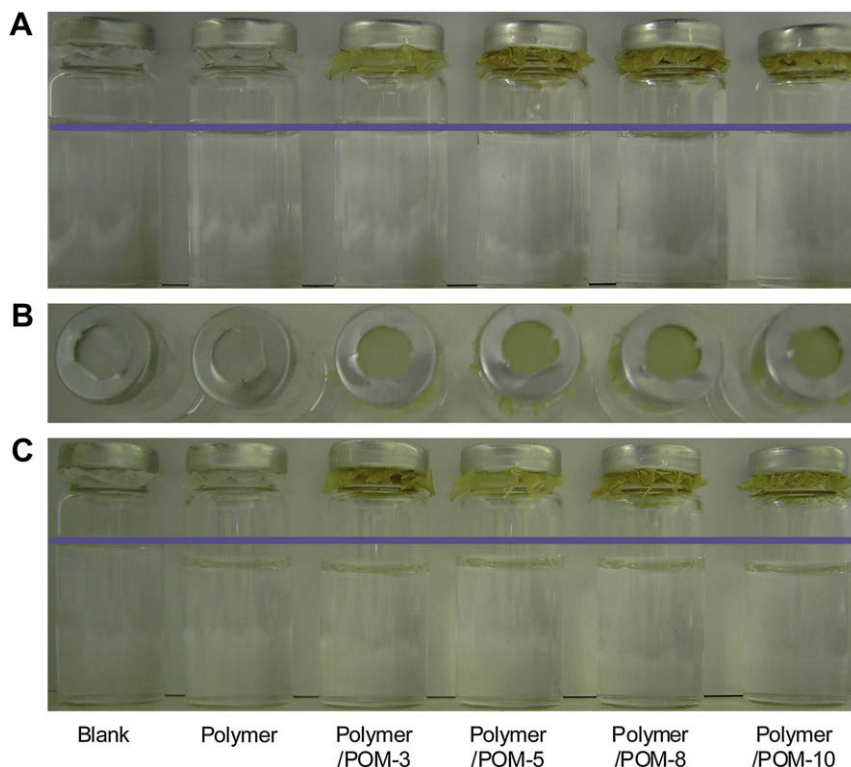


Fig. 2. (A) Photographs of the moisture vapor permeability of the Polymer/POM hybrid film and a control impermeable membrane (blank), (B) the moisture vapor transmission surface, (C) the results of moisture vapor permeability under 32 °C, 24 h.

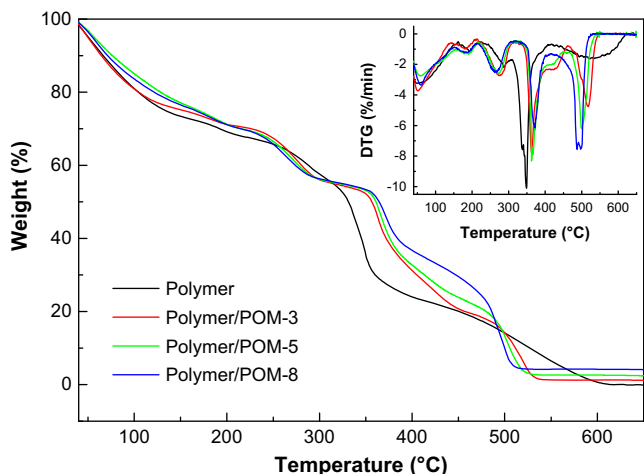


Fig. 3. TGA and DTG thermograms of the Polymer and Polymer/POM hybrids under nitrogen at the heating rate of 20 °C/min.

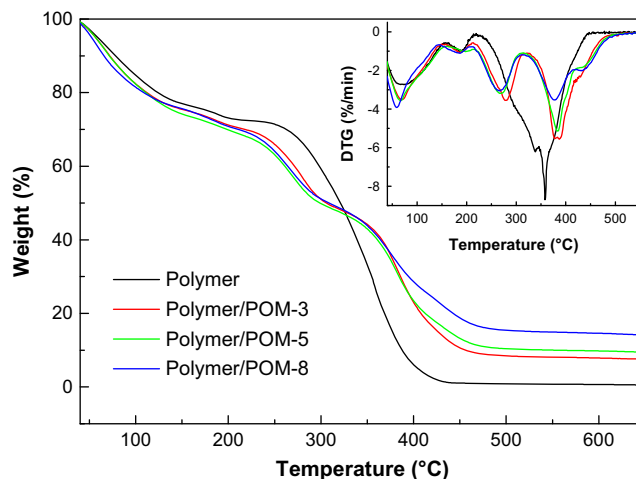


Fig. 4. TGA and DTG thermograms of the Polymer and Polymer/POM hybrids under air at the heating rate of 20 °C/min.

(<1 μm in diameter). This is characteristic of the facilitated transport mechanism, and clearly demonstrates that PEI functions efficiently as a carrier of vapor in the blend membrane. Chu and Yang investigated the effect of heat-treatment of a PVA membrane on water permeation through the membrane [28], and found that as the duration of heat-treatment increased, the density of the crosslinking formed by the condensation reaction between molecular chains increased, which resulted in a lower water permeation rate. This is attributable to the decrease in the pore size of PVA brought about by the increase in the crosslinking density. The TEM image of the Polymer/POM-8 hybrid solution showed non-agglomerated, scattered spherical POM particles at a low concentration, of sizes in the range of less than 20 nm (Fig. 1C). EDX analysis confirmed the existence of POM in the PVA/PEI matrix and qualitatively revealed the POM nanoparticle content.

The moisture vapor permeabilities, recorded in 24 h at 32 °C, of the control impermeable membrane and the Polymer/POM hybrid membranes are shown in Fig. 2 and the results are summarized in Table 1. In comparison with the value for the control membrane (0.8 g/m² h), the measured water vapor flux value was significantly increased for the Polymer/POM hybrid membranes (200.9–208.8 g/m² h) and was similar to that of the Polymer (PVA/PEI) film (200.6 g/m² h). The increased moisture vapor permeability of this material is attributable to the hydrophilic nature of the polymer matrix and the proposed hydrogen-bonded structure.

3.2. Thermal and redox properties

The weight-loss curves (TGA) and the differential thermogravimetry (DTG) of the PVA/PEI blend and the Polymer/POM hybrids, obtained at a heating rate of 20 °C/min under nitrogen, are shown in Fig. 3. The thermal decomposition temperatures in the

300–480 °C region were enhanced and in the 480–550 °C region were weakened for the Polymer/POM hybrids, and these effects increased with increasing POM content. On the other hand, the char yield (Y_c) in the degradation of the Polymer/POM hybrids was found to be proportional to the POM content. These results indicate that the thermal stability of the hybrid is influenced by the POM. This observation was further illustrated by the DTG curves obtained as a function of temperature. The weight loss below 200 °C is due to the degradation of water and small molecules, and the weight loss between 200 and 300 °C is attributed to the decomposition of hydrogen bonds between PVA and the PEI polymer. The weight loss in the intervals of 300–450 °C and 450–600 °C is attributed to the decomposition of the PEI and PVA units, respectively. Moreover, the

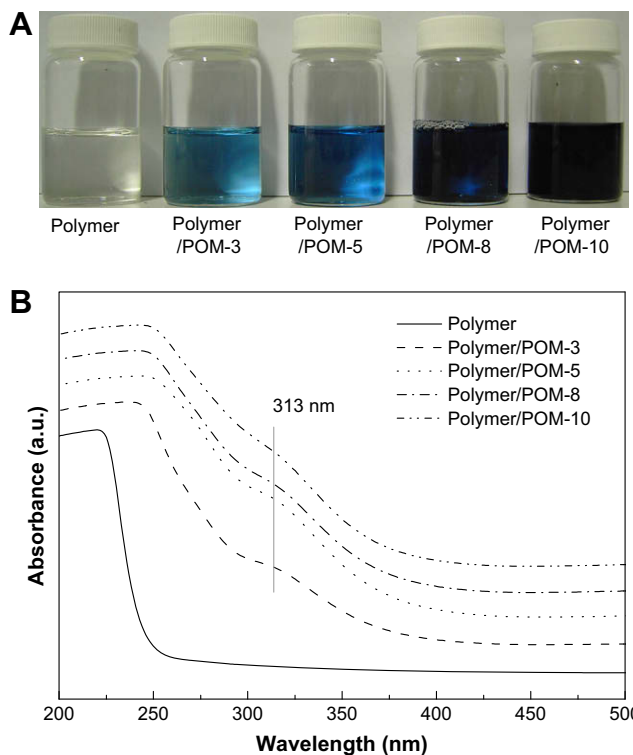


Fig. 5. (A) Photographs and (B) UV-Vis spectra of the reduced Polymer/POM hybrids.

Table 1
Results of moisture vapor permeability testing.

Sample	Weight (g)	Film area (cm ²)	Weight after 24 h (g)	Water vapor flux/32 °C (g/m ² h)
Blank	21.2409	1.1304	21.2388	0.8
Polymer	21.0475	1.1304	20.5034	200.6
Polymer/POM-3	21.1559	1.1304	20.6036	203.6
Polymer/POM-5	21.0400	1.1304	20.4950	200.9
Polymer/POM-8	20.9534	1.1304	20.3870	208.8
Polymer/POM-10	21.1101	1.1304	20.5606	202.5

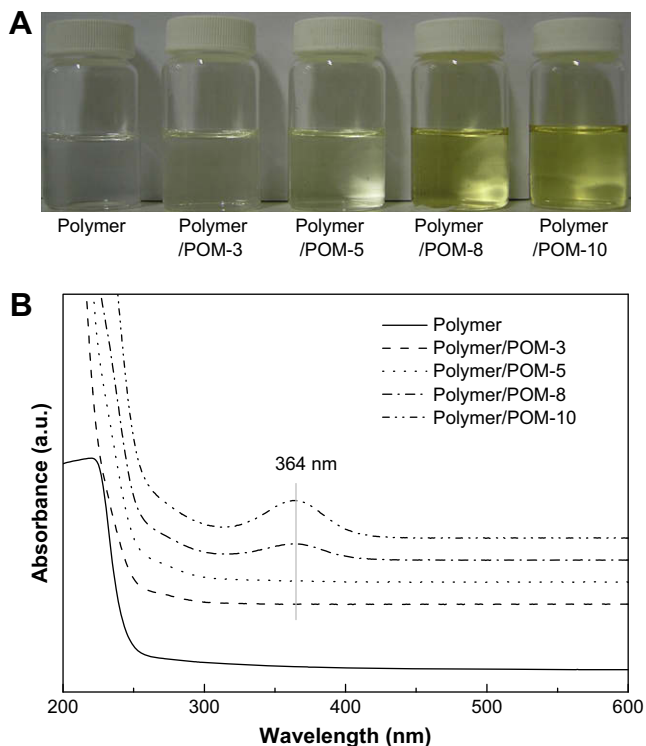


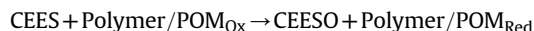
Fig. 6. (A) Photographs and (B) UV-Vis spectra of the oxidized Polymer/POM hybrids.

maximum rate of weight loss of the PEI units (300–450 °C) decreased with increasing POM content, while that of the PVA units (450–600 °C) increased. This observation reveals that the POM reduces the decomposition of the PEI polymer chain but enhances the decomposition of the PVA polymer chain.

Fig. 4 shows the TGA and DTG curves of the PVA/PEI blend and the Polymer/POM hybrids under air. The major mass loss of the PVA/PEI blend in the 200–430 °C region is attributed to the decomposition of the PVA–PEI crosslinking chains. It can be seen that the DTG curves of the Polymer/POM hybrids exhibit three clear stages in the 200–500 °C region, which can be attributed to the decomposition of the PEI (200–320 °C), PVA (320–430 °C), and

PVA–POM (430–500 °C) units, respectively. The weight loss in the 430–500 °C region, which is absent for the PVA/PEI blend, is mainly attributed to thermo-oxidative degradation of the PVA–POM units. Moreover, the degradation temperature of the PEI units is lower and the PVA units are higher as compared with those of the PVA/PEI blend. The DTG curves show that the POM weakens the rate of the scission of PVA chains, while the same rate of the PEI chains is almost constant. On the basis of the above observations, it is thought that the PVA chains with hydroxyl groups could exert chelating behavior, and this may be due to the coordination between O and the POM. Consequently, the thermo-oxidative stability of the hybrids was influenced by the inclusion of the inorganic component. Such a consequence may be due to the enhancement of heat transfer as a result of the increase in mobility of the POM, which leads to an increase in scission in the PEI chains, resulting in a reduction in scission within the PVA chains.

POM ($H_5PV_2Mo_{10}O_{40}$) detection of sulfides (e.g., CEES) can be explained by Eq. (1). The Polymer/POM oxidizes the sulfur atom of the sulfide, yielding Polymer/POM_{Red} and the oxidized form of the substrate (the sulfoxide, CEESO) [29].



V(V)system : orange blue (1)

The ease of oxidation of the sulfide depends on the nucleophilicity of the sulfur atom and the redox potential of the sulfide, and so, as expected, CEES, the closest electronic and structural model for HD, oxidizes the most slowly. Studies have shown that substitution of Mo^{6+} ions in Keggin structures owing to the higher electronegativity of V^{5+} ions often increases the oxidation ability of the POM [30]. Thus, the Polymer/POM exhibits a significant color change at ambient temperature in the detection step (Eq. (1)) with CEES.

Figs. 5 and 6 show photographs and the UV-Vis spectra of the Polymer/POM_{Red} and Polymer/POM_{Ox} hybrids: both exhibited UV absorption at approximately 313 nm for blue and approximately 364 nm for orange, respectively, the intensity distinctly increasing with increasing POM content. These bands are generally assigned to charge transfer from the bridging oxygen to the metal in polyoxometalates [31]. The POM used in this work, $H_5PV_2Mo_{10}O_{40}$, is of a type that contains a redox-active heteroatom. Catalysis by this complex proceeds exclusively via outer-sphere mechanisms,

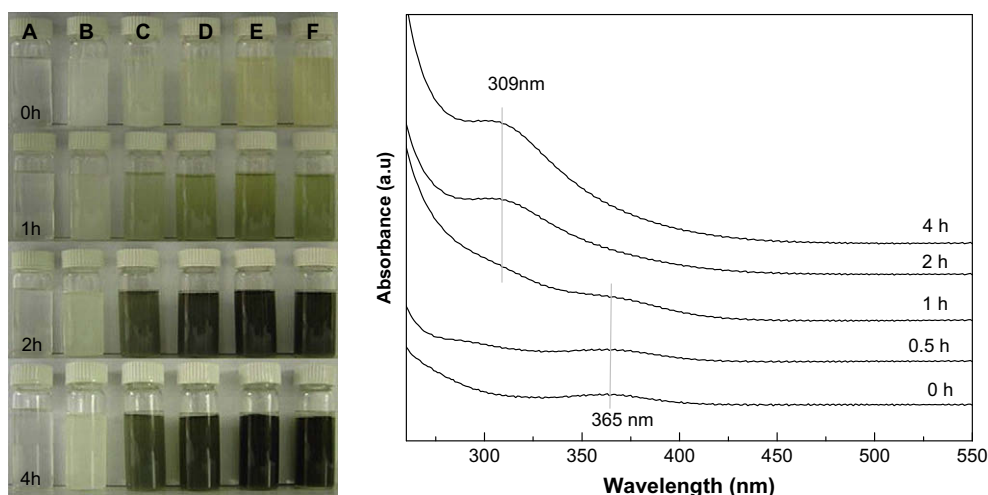


Fig. 7. Left, photographs of the oxidized test results in the different reaction time of (A) CEES, (B) Polymer + CEES, (C) Polymer/POM-3 + CEES, (D) Polymer/POM-5 + CEES, (E) Polymer/POM-8 + CEES, (F) Polymer/POM-10 + CEES; Right, UV-Vis spectra of the Polymer/POM-8 + CEES with different reaction time.

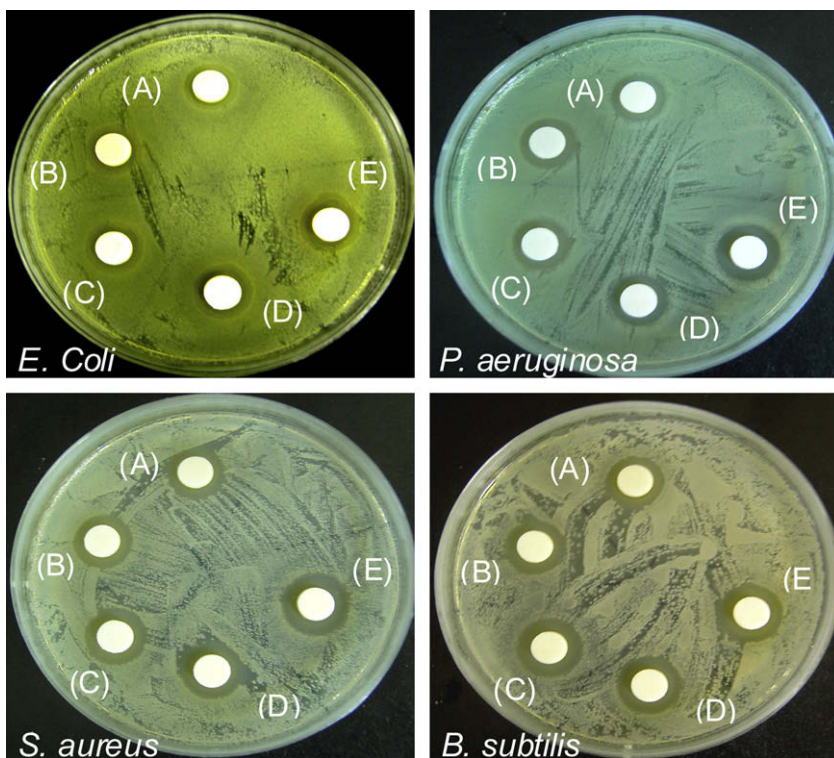


Fig. 8. Photographs of the antibacterial test results on these microbes in the systems of (A) Polymer, (B) Polymer/POM-3, (C) Polymer/POM-5, (D) Polymer/POM-8 and (E) Polymer/POM-10.

because the V(V) is buried in the center of the POM structure [10]. When added to the Polymer/POM solution, CEES was oxidized by the POM, as indicated by a dramatic change from orange to blue in ca. 1 h (Fig. 7, left). The difference in the UV–Vis spectra of the oxidized and reduced forms of the POM in solution is shown in Fig. 7.

3.3. Antibacterial effects

The antibacterial efficacies of the Polymer/POM hybrids against bacteria were assessed based on zone of inhibition testing, MIC and the plate-counting method. Fig. 8 and Table 2 detail the relative retention of activity (zone of inhibition) of the Polymer and the Polymer/POM hybrids against bacteria. After 24 h of incubation, the zones of inhibition of the Polymer/POM hybrids against bacteria ranged from 10.21 to 16.05 mm and were larger than that of the Polymer blend (10.17–14.30 mm). The Polymer blend and Polymer/POM hybrids exhibited significant efficacy against bacteria, especially against Gram-positive *S. aureus* and *B. subtilis*, and the efficacy increased with increasing POM content. The results in Table 3 show that the hybrids have good efficacy against these bacteria. The MIC values of the Polymer/POM hybrids against bacteria were 0.02–20 $\mu\text{g}/\text{mL}$ and were lower than that of the Polymer blend (2–20 $\mu\text{g}/\text{mL}$). Thus, it is likely that the highly-negative charge of the POM

stimulates the cell to result in facilitation of the bacterial morphological change from bacillary form to coccid form, reflecting bacterial death [19].

Fig. 9 shows the number of bacterial colonies grown on MH plates as a function of the amount of Polymer/POM-8 hybrid when approximately 10^7 CFU of *S. aureus* were applied to the plates. The size of the bacterial colonies grown on plates with more than 50 mg of Polymer/POM-8 particles was significantly reduced, and the antibacterial performance would therefore be improved greatly with increasing amounts of Polymer/POM-8 particles. The dynamics of bacterial growth were also monitored in MH medium supplemented with 10^7 CFU *S. aureus* cells and with 50 mg of Polymer/POM-8 under different inoculation durations. Fig. 10 demonstrates that the bacterial colonies of Gram-positive *S. aureus* were completely killed after 24 h of inoculation and the percentage reduction of bacteria was approximately 100% after 8–48 h of inoculation. The mechanism of the antibacterial activity of the POM against the Gram-negative strains is considered to be as follows: the fluorescent X-ray analysis results showed uptake of the POM into the bacterial cell. The Gram-negative strains can take the hydrophilic compounds into the periplasmic space through the porin protein, which is a pore-forming protein working towards the penetration of the hydrophilic compound in the outer membrane [19].

Table 2
Zone of inhibition (mm) against bacteria of the Polymer and Polymer/POM hybrids.

Bacteria	Polymer	Polymer/ POM-3	Polymer/ POM-5	Polymer/ POM-8	Polymer/ POM-10
<i>E. coli</i>	10.17	10.21	10.60	11.20	11.58
<i>P. aeruginosa</i>	12.55	13.38	13.75	13.80	14.79
<i>S. aureus</i>	14.30	14.35	15.07	15.38	15.73
<i>B. subtilis</i>	13.47	14.17	15.10	15.43	16.05

Table 3
The MIC ($\mu\text{g}/\text{mL}$) values of the Polymer and Polymer/POM hybrids on bacteria.

Bacteria	Polymer	Polymer/ POM-3	Polymer/ POM-5	Polymer/ POM-8	Polymer/ POM-10
<i>E. coli</i>	20	20	2	2	2
<i>P. aeruginosa</i>	2	2	0.2	0.2	0.2
<i>S. aureus</i>	2	0.2	0.2	0.02	0.02
<i>B. subtilis</i>	2	2	0.2	0.2	0.2

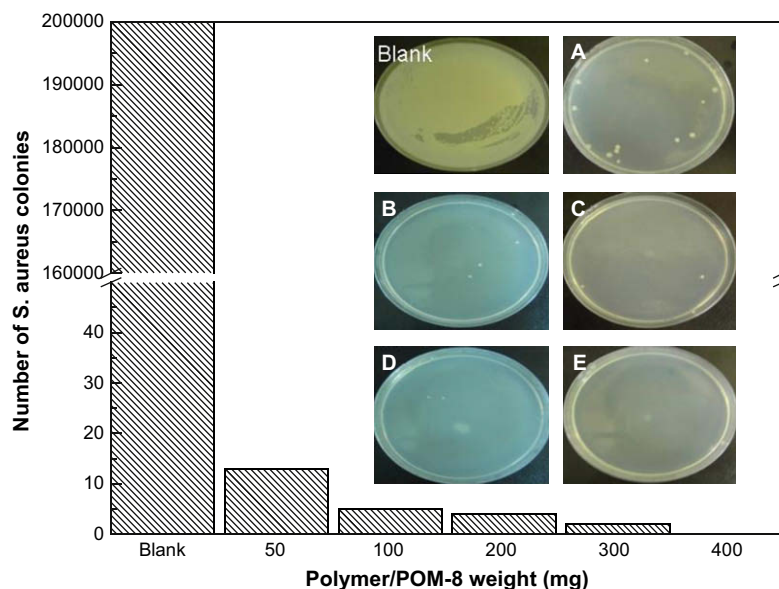


Fig. 9. Number of *S. aureus* colonies as a function of the weight of Polymer/POM-8 hybrid put into 10^7 CFU of bacterial colonies. The inserted photograph of MH plates incubated under the condition in Fig. 9: (A) 50, (B) 100, (C) 200, (D) 300 and (E) 400 mg.

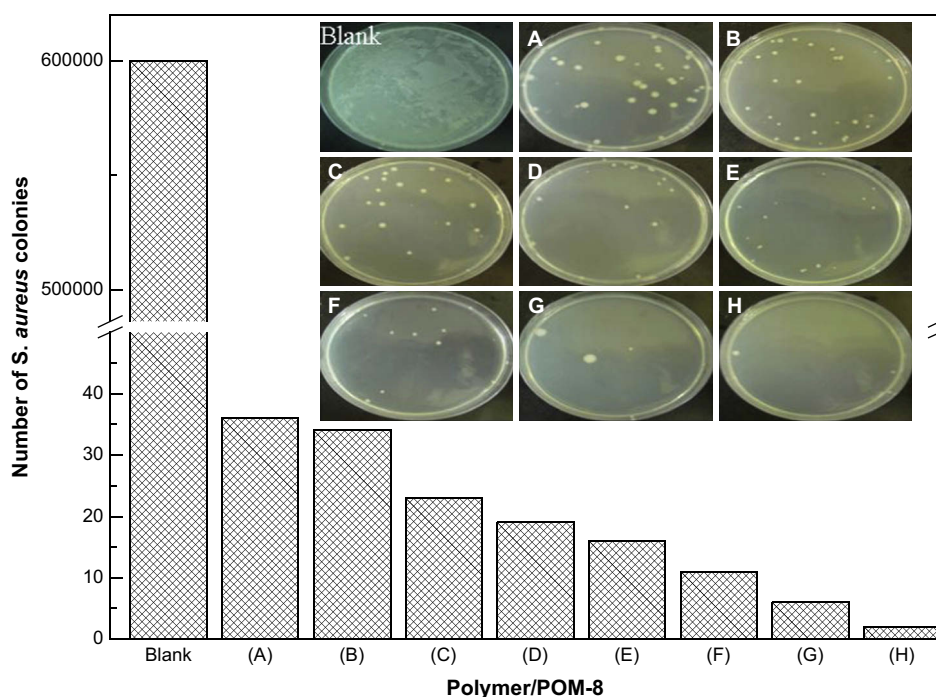


Fig. 10. Number of *S. aureus* colonies as a function of the inoculation time of Polymer/POM-8 (50 mg) put into 10^7 CFU of bacterial colonies. The inserted photograph of MH plates incubated under the condition in Fig. 10: (A) 0.5 h, (B) 2 h, (C) 4 h, (D) 8 h, (E) 12 h, (F) 24 h, (G) 36 h and (H) 48 h.

4. Conclusions

The results of this study show that POM nanoparticle-doped PVA/PEI blend systems are capable of destroying CEES and bacteria while allowing moisture vapor permeability. The substitution of two vanadium atoms into the Mo_{12} framework, as exhibited by $\text{H}_5\text{PV}_2\text{Mo}_{10}\text{O}_{40}$, provides additional redox capability. When CEES comes into contact with the Polymer/POM hybrids, the hybrids change from orange to blue in ca. 1 h at ambient temperature, exhibiting a potential HD-detecting capability. These Polymer/POM

hybrids possess excellent antibacterial abilities: their antibacterial performance against Gram-negative *E. coli* and *P. aeruginosa*, and Gram-positive *S. aureus* and *B. subtilis*, was investigated by zone of inhibition testing, MIC and the plate-counting method, and the results showed that the Polymer/POM hybrids exhibit strong antibacterial activity against these bacteria. The lowest values of MIC for the PVA/PEI blend and the Polymer/POM hybrids were 2 and 0.02 $\mu\text{g}/\text{mL}$, respectively. The structure and negatively-charged anion characteristics of the POM are important in the antibacterial activity against Gram microbes. Further study is still needed in

order to validate that these material systems are robust enough to survive the military environment, but the initial test results are very positive. If successful, these materials have the potential to meet the holy grail of protective materials, a self-detoxifying material.

Acknowledgement

The authors thank the National Science Council of the Republic of China for supporting this work (Grant NSC 96-2113-M-606-003-MY3).

References

- [1] International Patent Application no PCT/GB03/00271. 2004.
- [2] Yu DG, Lin WC, Lin CH, Chang LM, Yang MC. *Mater Chem Phys* 2007;101:93.
- [3] Rajendran S, Sivakumar M, Subadevi R. *Mater Lett* 2004;58:641.
- [4] Yang YC, Baker JA, Ward JR. *Chem Rev* 1992;92:1729.
- [5] Liu HI, Iglesia E. *J Catal* 2004;223:161.
- [6] Vazylyev M, Dorit SR, Haimov A, Maayan G, Neumann R. *Top Catal* 2005;34:93.
- [7] Hill CL. *J Mol Catal A Chem* 2007;262:2.
- [8] Erik DC. *Rev Med Virol* 2000;10:255.
- [9] Erik DC. *Med Res Rev* 2002;22:531.
- [10] Johnson RP, Hill CL. *J Appl Toxicol* 1999;19:571.
- [11] Hill CL, Gall RD. *J Mol Catal A Chem* 1996;114:103.
- [12] Gall RD, Hill CL, Walker JE. *J Catal* 1996;159:473.
- [13] Judd DA, Nettles JH, Nevins N. *J Am Chem Soc* 2001;123:886.
- [14] Chen CN, Lin CPC, Huang KK. *Alternative Med* 2005;2:209.
- [15] Zhai HJ, Liu SX, Li YX. *Chin J Inorg Chem* 2005;21:1798.
- [16] Yamase T. In: Salamone JC, editor. *Polymeric materials encyclopedia: synthesis, properties, and applications*. Boca Raton, FL: CRC Press; 1996. p. 365.
- [17] Hill CL. *Chem Rev* 1998;98:1.
- [18] Fukuda N, Yamase T, Tajima Y. *Biol Pharm Bull* 1999;22:463.
- [19] Inoue M, Segawa K, Matsunaga S, Matsumoto N, Oda M, Yamase T. *J Inorg Biochem* 2005;99:1023.
- [20] Hu DH, Shao C, Guan W, Su ZM, Sun JH. *J Inorg Biochem* 2007;101:89.
- [21] Shigeta S, Yamase T. *Antivir Chem Chemother* 2005;16:23.
- [22] Shigeta S, Mori S, Yamase T, Yamamoto N. *Biomed Pharmacother* 2006;60:211.
- [23] Wagner GW, Koper OB, Lucas E, Decker S, Klabunde KJ. *J Phys Chem* 2000;B 104:5118.
- [24] Koper O, Klabunde KJ, Marchin G, Stormenov P, Bohra L. *Curr Microbiol* 2002;44:49.
- [25] Hoskin FCG, Steeves DM, Walker JE. *Biol Bull* 1999;197:284.
- [26] Damyanova S, Gomez LM, Banares MA, Fierro JLG. *Chem Mater* 2000;12:501.
- [27] Dong DW, Yang YS, Jiang BZ. *Mater Chem Phys* 2006;95:90.
- [28] Chu TJ, Yang MH. *Membrane* 1992;17:263.
- [29] Okun NM, Anderson TM, Hill CL. *J Mol Catal A Chem* 2003;197:283.
- [30] Wang JY, Hu CW, Jian M, Li GY. *J Catal* 2006;240:23.
- [31] Hill CL, Bouchard DA, Kadkhodayan M, Williamson MM, Schmidt JA, Hilinski EF. *J Am Chem Soc* 1998;110:5471.